Tuning thermal conductivity in homoepitaxial $SrTiO_3$ films via defects

Charles M. Brooks, Richard B. Wilson, Anna Schäfer, Julia A. Mundy, Megan E. Holtz, David A. Muller, Jürgen Schubert, David G. Cahill, and Darrell G. Schlom

Citation: Appl. Phys. Lett. **107**, 051902 (2015); doi: 10.1063/1.4927200
View online: http://dx.doi.org/10.1063/1.4927200
View Table of Contents: http://aip.scitation.org/toc/apl/107/5
Published by the American Institute of Physics

Tuning thermal conductivity in homoepitaxial $SrTiO_3$ films via defects

Charles M. Brooks,[1,2] Richard B. Wilson,[3] Anna Schäfer,[4] Julia A. Mundy,[5] Megan E. Holtz,[5] David A. Muller,[5,6] Jürgen Schubert,[4] David G. Cahill,[3] and Darrell G. Schlom[1,6]

[1]*Department of Materials Science and Engineering, Cornell University, Ithaca, New York 14853-1501, USA*
[2]*Department of Materials Science and Engineering, Pennsylvania State University, University Park, Pennsylvania 16802, USA*
[3]*Department of Materials Science and Engineering and Materials Research Laboratory, University of Illinois, Urbana, Illinois 61801, USA*
[4]*Peter Grünberg Institute (PGI9-IT), JARA-Fundamentals of Future Information Technology, Research Centre Jülich, D-52425 Jülich, Germany*
[5]*School of Applied and Engineering Physics, Cornell University, Ithaca, New York 14853, USA*
[6]*Kavli Institute at Cornell for Nanoscale Science, Ithaca, New York 14853, USA*

(Received 31 May 2015; accepted 19 June 2015; published online 5 August 2015)

We demonstrate the ability to tune the thermal conductivity of homoepitaxial $SrTiO_3$ films deposited by reactive molecular-beam epitaxy by varying growth temperature, oxidation environment, and cation stoichiometry. Both point defects and planar defects decrease the longitudinal thermal conductivity (k_{33}), with the greatest decrease in films of the same composition observed for films containing planar defects oriented perpendicular to the direction of heat flow. The longitudinal thermal conductivity can be modified by as much as 80%—from 11.5 W $m^{-1}K^{-1}$ for stoichiometric homoepitaxial $SrTiO_3$ to 2 W $m^{-1}K^{-1}$ for strontium-rich homoepitaxial $Sr_{1+\delta}TiO_x$ films—by incorporating $(SrO)_2$ Ruddlesden-Popper planar defects. © *2015 AIP Publishing LLC*.
[http://dx.doi.org/10.1063/1.4927200]

The ability to control thermal conductivity is important to numerous applications. For instance, improvements to both oxide thermal barrier coatings and thermoelectrics hinge on engineering a thermally resistive material that is optimized in conjunction with other parameters such as thermal expansion, microstructure, toughness, or carrier mobility. The phenomenal adaptability of perovskites to incorporate a majority of the elements in the periodic table provides for a broad variation of properties based on elemental selection alone. Because this compositional tunability is accompanied by high-temperature stability, oxide materials in the perovskite family hold promise for thermal barrier[1] and thermoelectric applications.[2,3]

The quintessential perovskite oxide, $SrTiO_3$, exhibits many of the useful properties found in oxide materials and provides a rich experimental parameter space since defects are easily accommodated into the structure as point defects[4,5] or planar defects, where the latter are in the form of Ruddlesden-Popper (RP) planar faults.[6–10] These RP phases have been suggested as a pathway to achieving thermal barrier coatings using $SrTiO_3$-based materials.[11] *N*-type $SrTiO_3$ has itself been proposed as a candidate for high-temperature thermoelectric applications.[12] Doped epitaxial films of $SrTiO_3$ have a figure of merit (*ZT*) of 0.28 at 873 K.[13] In order to improve the *ZT* of thermoelectrics, attempts are often made to reduce the thermal conductivity without detrimentally influencing the electrical conductivity and Seebeck coefficient. Altering the microstructure of the material or introducing point defects can achieve this;[14] the introduction of RP planar faults may also be a route to *ZT* enhancement,[11] though negligible enhancement of *ZT* has been found in bulk.[15,16]

Small deviations in growth conditions have been shown to influence the thermal conductivity of epitaxial $SrTiO_3$ thin films.[17] The thermal conductivity of $SrTiO_3$ films grown by pulsed-laser deposition (PLD) has been observed to vary by a factor of three with laser fluence, which also affects other film attributes including composition.[18]

Here, we demonstrate the ability to tune thermal conductivity by controlling the formation of defects in homoepitaxial films grown by reactive molecular-beam epitaxy (MBE).[19] This is achieved by varying the substrate temperature, oxidation environment, and incident flux ratio between molecular beams of the constituent elements during the deposition process. Due to the independent control of growth parameters available when depositing films by MBE, we are able to isolate the effect of film stoichiometry from other variables. We observe reductions in thermal conductivity of $Sr_{1+\delta}TiO_x$ films by as much as ~80% compared with stoichiometric $SrTiO_3$. This significant reduction occurs when RP planar faults[6–8] (a syntactic intergrowth of an extra plane of SrO) form perpendicular to the growth direction. We note that the orientation of the RP defects depends on growth temperature as well as film composition.

When it comes to assessing the perfection of semiconductor materials, measurements of transport properties can be far more sensitive than structural characterization. For this reason, electrical mobility at low temperature is commonly used to assess the quality of lightly doped semiconductors[20,21] or two-dimensional electron gasses.[22] Thermal conductivity, another transport property, is a useful metric for assessing the crystalline quality of thin films with high-quality films of sufficient thickness reproducing the thermal conductivity observed in bulk single crystals.[17] We studied the thermal conductivity of the films along the direction perpendicular to the (001) $SrTiO_3$ substrate surface (k_{33}), referred to as the longitudinal thermal conductivity,[23] by time-domain thermoreflectance (TDTR).[17]

Stoichiometric $SrTiO_3$ films, independent of the film deposition temperature, do not exhibit x-ray diffraction (XRD) reflections distinct from those originating from the underlying $SrTiO_3$ substrate. This is shown in the θ–2θ XRD scans displayed in Fig. 1(a) indicating the out-of-plane lattice constant of the stoichiometric films grown by MBE and bulk $SrTiO_3$ substrate are identical within the resolution of the measurement, which are limited by overlapping film and substrate reflections. The films with non-stoichiometric strontium content ($\delta \neq 0$) deposited at 800 °C are shown in Fig. 1(b); the θ–2θ scan of one of the samples ($\delta = 0.25$) is plotted over a wider range in Fig. 1(c).

The many peaks in Fig. 1(c) can be indexed with a single c-axis length of ~35.8 ± 0.2 Å, which is about the value of the $n = 4$ $Sr_{n+1}Ti_nO_{3n+1}$ phase, i.e., $Sr_5Ti_4O_{13}$. This phase has a composition consistent with $\delta = 0.25$. An important difference, however, is that single-phase $Sr_5Ti_4O_{13}$ contains a glide plane half way up its unit cell, resulting in destructive interference and the absence of all odd 00ℓ peaks.[24] In contrast, many of the intense peaks in Fig. 1(c) have odd indices, making the observed XRD pattern inconsistent with single-phase $Sr_5Ti_4O_{13}$. This observation is reminiscent of unusual XRD patterns seen in the growth of "$Bi_2Sr_2Ca_{n-1}Cu_nO_{2n+4}$" films,[25–30] where again both even and odd 00ℓ peaks were used to index the observed XRD patterns even though odd peaks are systematically absent in all known $Bi_2Sr_2Ca_{n-1}Cu_nO_{2n+4}$ phases because they contain a glide plane half way up their unit cells. The explanation revealed by XRD simulations[28,29] and TEM[28] on the unusual "$Bi_2Sr_2Ca_{n-1}Cu_nO_{2n+4}$" films was that they consisted of layering disorder,[31–33] i.e., syntactic intergrowths of $Bi_2Sr_2Ca_{n-1}Cu_nO_{2n+4}$ phases; the same explanation is likely for our $\delta = 0.25$ film.

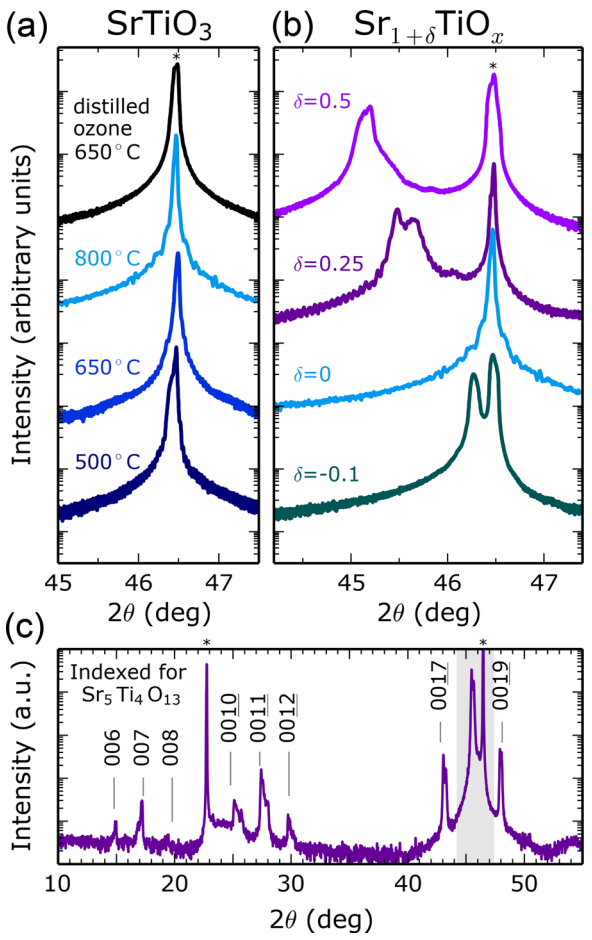

FIG. 1. (a) θ–2θ XRD spectra of the 002 peaks of stoichiometric $SrTiO_3$ films deposited at different temperatures in 10% ozone and at 650 °C in distilled ozone. (b) θ-2θ XRD spectra of strontium-excess $Sr_{1+\delta}TiO_x$ films deposited at 800 °C. (c) A θ-2θ XRD scan over a wider region reveals RP phase peaks that can be indexed as $Sr_5Ti_4O_{13}$ ($n = 4$) with both even and odd 00ℓ peaks due to the presence of significant layering disorder.

All non-stoichiometric $SrTiO_3$ films show film 002 peaks at lower 2θ angle than the substrate 002 peak, signifying an apparent expansion of the out-of-plane lattice constant of the film relative to the substrate. This is commonly seen in non-stoichiometric $SrTiO_3$ films.[34,35] The apparent out-of-plane lattice constants for the films, shown in Fig. 2, were calculated from the XRD results. Strontium excess samples ($\delta > 0$) display a large increase in this c-axis lattice constant. In Fig. 2, these results are shown alongside calculated values for the apparent or pseudocubic c-axis lattice constant for the RP series of $Sr_{n+1}Ti_nO_{3n+1}$ films. This value is calculated according to $c = 2(n \times a_{STO} + d_{SrO\text{-}SrO})/(2n + 1)$, where a_{STO} is the $SrTiO_3$ lattice constant and $d_{SrO\text{-}SrO}$ is the average SrO bilayer distance in the RP phases.[36] In addition to these lattice constants from the RP series, Fig. 2 includes estimated values for a mixture of RP planar faults for the same composition, but distributed evenly along the out-of-plane c-axis and the in-plane a and b axes as well. Such a distribution would reduce the out-of-plane lattice expansion by a factor of three. If the lattice expansion observed in these films is solely due to the inclusion of RP planar faults, then the RP phases should represent the upper limit. All of the Sr-excess films in this study fall below this upper boundary indicating that alignment of planar faults along the growth direction can more than account for all observed lattice expansion in these films.

Bright-field images of the $\delta = 0.25$ film deposited at 800 °C, shown in Figs. 3(a) and 3(b), reveal that the film has RP planar faults that appear to primarily lie in the plane parallel to the substrate and perpendicular to the film growth direction. This alignment and tendency to order in a periodic

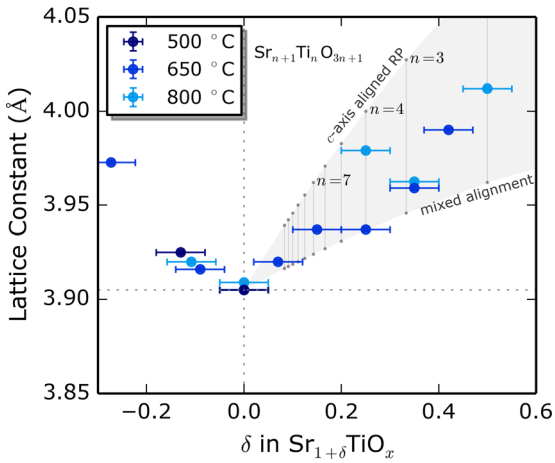

FIG. 2. The apparent out-of-plane or c-axis lattice constant measured by XRD for $Sr_{1+\delta}TiO_x$ films versus Sr:Ti stoichiometry ratio determined by RBS. Both the pseudocubic c-axis lattice constant of the RP phases of $Sr_{n+1}Ti_nO_{3n+1}$ up to $n = 12$ and the expected apparent lattice constant for a RP phase of mixed alignment for the same composition are plotted for comparison.

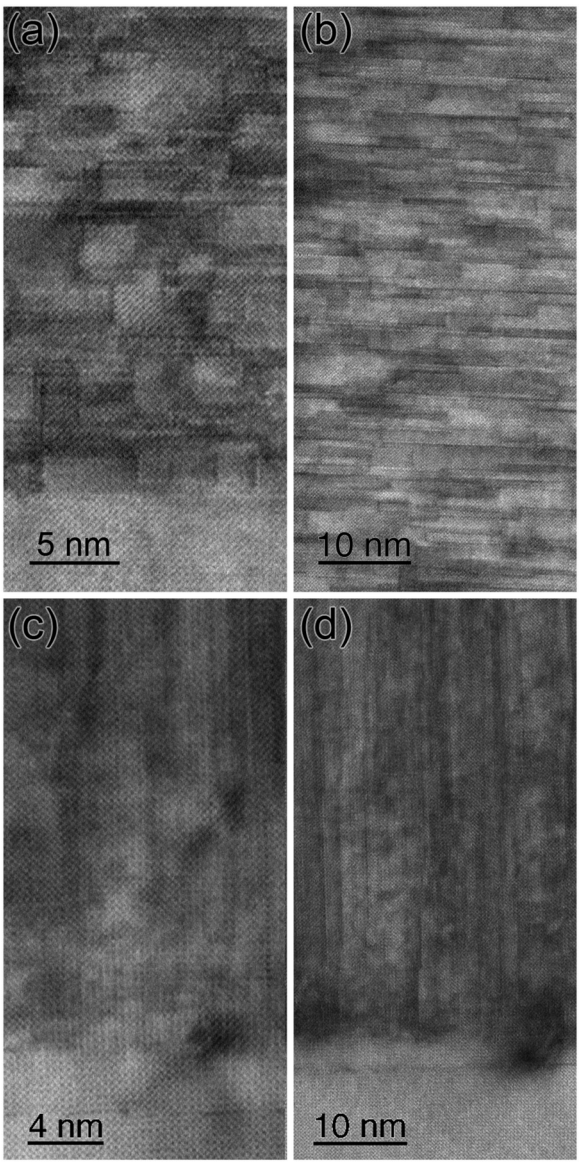

FIG. 3. Bright-field STEM images taken at different magnifications (a) and (b) of the film with $\delta = 0.25$ grown at 800 °C. (c) and (d) show images of the sample with $\delta = 0.25$ deposited at 650 °C. The excess strontium is clearly seen to form layers perpendicular to the growth direction at high temperature in (b) and parallel to the growth direction in (d).

manner were observed to occur for films deposited at the highest temperature, as evidenced by the presence of superlattice type reflections in the XRD data, displayed in Fig. 1(c). This periodic ordering along the growth direction has been seen in $n = 1$ (Sr_2TiO_4) films deposited at high-temperature by other techniques[37] and in other RP forming compositions.[38–43] A strontium-rich sample deposited at a lower temperature of 650 °C is shown in Figs. 3(c) and 3(d) appears to mostly contain planar faults perpendicular to the in-plane directions instead of the growth direction, in contrast to the film deposited with the same composition at 800 °C. This demonstrates the ability to control RP fault orientation with growth temperature. The RP planar faults predominantly form perpendicular to the growth direction when a film with excess strontium is deposited at the relatively higher temperature of 800 °C, thus approaching an intentionally ordered *c*-axis oriented RP film (e.g., $Sr_{n+1}Ti_nO_{3n+1}$) of equivalent composition. Some alignment of these faults has been observed previously in non-stoichiometric $Sr_{1+\delta}TiO_x$ samples deposited through source shuttering at 650 °C.[34] Of course, deliberately shuttering extra SrO planes into stoichiometric $SrTiO_3$ is an effective way of introducing RP faults along the growth direction,[24,44] and has been used to make $Sr_{n+1}Ti_nO_{3n+1}$ phases with n as high as 10.[45] Such a method is not employed, however, in the work described here. Partial orientation of RP faults has also been attributed to composition changes achieved through controlling laser fluence in PLD.[46] No such ordering of defects is observed for strontium-poor samples. A disordered appearance in the bright-field image is commonly observed in strontium deficient films,[34,47] and consistent with the presence of high concentrations of point defects.

Figure 4(a) shows a comparison between the temperature, at which the films were grown, and the longitudinal thermal conductivity of $SrTiO_3$ films determined to be stoichiometric to within ±5% by RBS. Interestingly, these films appear to have the same out-of-plane lattice constant by XRD, yet vary in film longitudinal thermal conductivity by as much as 4 W/m·K depending on growth temperature and oxygen background pressure. Growth temperature has been reported to affect both film lattice constant and thermal conductivity in homoepitaxial $SrTiO_3$ films deposited by sputtering.[48] For a comparable range of temperatures, our results show a similar though lesser effect (~30%) without the clear difference in out-of-plane lattice constants from XRD. The stoichiometric film deposited in distilled ozone (~80% O_3) at 650 °C shows the highest longitudinal thermal conductivity, 11.5 W/m·K at room temperature. It is higher than the samples deposited in the less oxidizing environment of ~10% ozone. In addition, post-growth annealing of the samples in 1 atm of O_2 at 700 °C for 1 h failed to consistently improve the film longitudinal thermal conductivity, suggesting that the defects involved in films grown under less oxidizing conditions are not simply oxygen vacancies, but rather defect complexes that also involve cation species (which have much lower diffusion coefficients than oxygen[49]). Growing with ~10% ozone instead of distilled ozone resulted in a ~23% reduction in longitudinal thermal conductivity. Reductions as high as ~32% have been observed in reduced bulk $SrTiO_3$.[50] Even larger reductions in longitudinal thermal conductivity of oxygen-deficient $SrTiO_3$ films grown by PLD have been observed,[18] but low growth pressures in PLD also alter the plasma and bombardment effects, thus complicating the interpretation as being purely due to oxygen-related defects.[51]

The dependence of longitudinal thermal conductivity on film composition is displayed in Fig. 4(b). The longitudinal thermal conductivity of the $\delta = 0.25$ film deposited at 800 °C is comparable to that of a phase-pure $n = 4$ RP film, while also sharing a similar overall film composition.[52] Simulations predict that the minimum in the longitudinal thermal conductivity as a function of n in $Sr_{n+1}Ti_nO_{3n+1}$ phases occurs at $n = 5$ for heat transport perpendicular to the RP planar faults.[11] Note that the distance between RP planar faults in an $n = 4$ RP phase is about 1.8 nm, which is in the range of 1–3 nm, where the minimum in longitudinal thermal conductivity has been observed in other layered heterostructures, including related oxides.[53,54] Superlattices and bulk

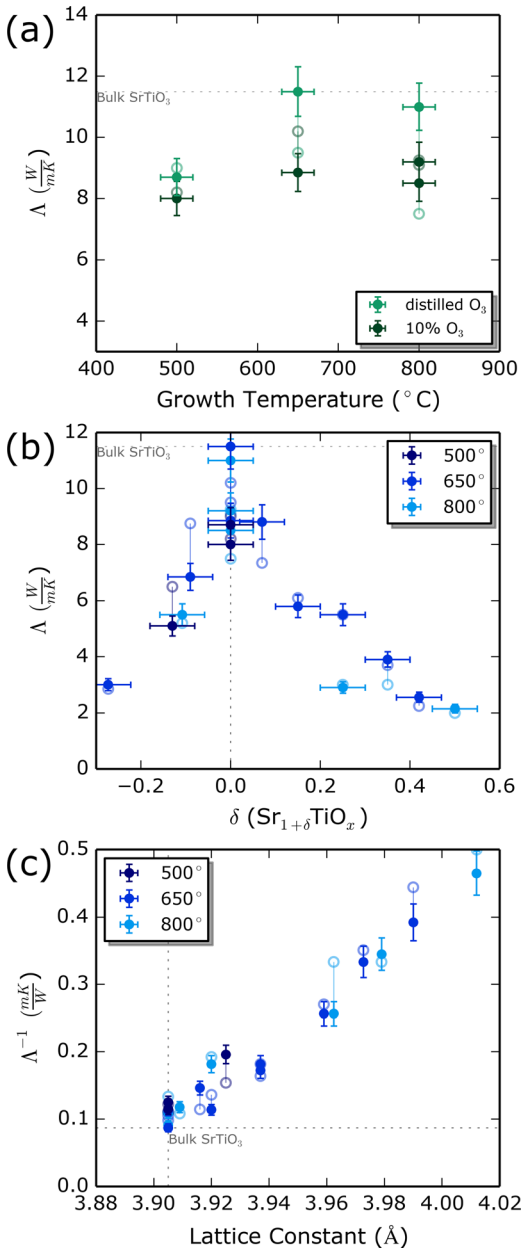

FIG. 4. (a) The longitudinal thermal conductivity of the same stoichiometric $SrTiO_3$ samples, as shown in Fig. 1(a). (b) The dependence of longitudinal thermal conductivity in relation to film composition with excess strontium films showing the largest decrease. (c) The longitudinal thermal resistivity versus the apparent out-of-plane lattice constant of the film. The open circles correspond to measurements of the same films following a 700 °C anneal in 1 atm of oxygen for 1 h. Multiple TDTR measurements taken in different sample areas were found to be consistent. The vertical-axis error bars for sample thermal conductivity were determined from the uncertainties in the TDTR measurement.

$Sr_{n+1}Ti_nO_{3n+1}$ RP phases with $n=1$ and $n=2$ also exhibit reduced thermal conductivity (k_{33}) compared with bulk stoichiometric $SrTiO_3$.[55] RP planar defects in films significantly decrease the longitudinal thermal conductivity when aligned perpendicular to the growth direction. Films deficient in strontium show a reduction in longitudinal thermal conductivity of ~30% on average when compared with stoichiometric samples, similar to other studies.[18] These strontium deficient samples show the largest increase in longitudinal thermal conductivity following an anneal in oxygen (700 °C for 1 h in 1 atm of O_2).

Although the films in this study were grown by MBE, the growth conditions should be adaptable to other growth methods as well since the ~80% reduction in longitudinal thermal conductivity observed primarily depends on the presence of excess strontium forming RP faults and does not rely on features unique to MBE such as individual source shuttering. This should allow for $Sr_{1+\delta}TiO_x$ films of low thermal conductivity to be deposited by alternative deposition methods. These results imply that the longitudinal thermal conductivity of other perovskite systems may be similarly reduced through the introduction of RP faults. Further, although electrical conductivity measurements were not part of this study, steps may be taken to increase the electrical conductivity of $Sr_{1+\delta}TiO_x$ samples, such as doping with niobium, lanthanum, or oxygen vacancies, as has been used to increase the conductivity of $Sr_{n+1}Ti_nO_{3n+1}$ RP phases in both bulk[56] and thin film form.[39,57,58]

In summary, we have shown the dependence of longitudinal thermal conductivity on growth temperature and oxidation environment for stoichiometric $SrTiO_3$ films deposited by MBE, all of which display no detectable change in film lattice constant. We also observed a significant reduction of ~80% in longitudinal thermal conductivity in $Sr_{1+\delta}TiO_x$ films ($\delta = 0.25$–0.5) through the introduction of a significant concentration of RP planar faults. Some evidence for the ordering of these faults is seen for films deposited at 800 °C, but the ordering is not necessary to achieve a significant reduction in longitudinal thermal conductivity. These results provide an avenue for minimizing longitudinal thermal conductivity in films of $SrTiO_3$ or related perovskites for applications in areas such as thermal barrier coatings and high-temperature thermoelectrics.

We gratefully acknowledge the financial support from the National Science Foundation through the MRSEC program (Nos. DMR-1420620 and DMR-1120296). This work was performed in part at the Cornell NanoScale Facility, a member of the National Nanotechnology Infrastructure Network, which was supported by the National Science Foundation (Grant No. ECCS-0335765). The portion of the electron microscopy completed by M.E.H. was supported by the US Department of Energy, Basic Energy Science under Award No. DE-SCOO02334. J.A.M. acknowledges financial support from the Army Research Office in the form of a National Defense Science & Engineering Graduate Fellowship and from the National Science Foundation in the form of a graduate research fellowship. Thermal conductivity measurements were supported by AFOSR Contract No. AF FA9550-12-1-0073 and carried out in part in the Frederick Seitz Materials Research Laboratory Central Research Facilities, University of Illinois. R.B.W. acknowledges the Department of Defense for the National Defense Science and Engineering Graduate Fellowship that supported him during this work.

[1]R. Vassen, X.-Q. Cao, F. Tietz, D. Basu, and D. Stöver, J. Am. Ceram. Soc. **83**, 2023–2028 (2000).
[2]J. W. Fergus, J. Eur. Ceram. Soc. **32**, 525–540 (2012).
[3]A. Weidenkaff, R. Robert, M. Aguirre, L. Bocher, T. Lippert, and S. Canulescu, Renewable Energy **33**, 342–347 (2008).
[4]T. Tanaka, K. Matsunaga, Y. Ikuhara, and T. Yamamoto, Phys. Rev. B **68**, 205213 (2003).

[5]D. Freedman, D. Roundy, and T. Arias, Phys. Rev. B **80**, 064108 (2009).
[6]D. Balz and K. Plieth, Z. Elektrochem. **59**, 545–551 (1955).
[7]S. N. Ruddlesden and P. Popper, Acta Cryst. **10**, 538–539 (1957).
[8]S. N. Ruddlesden and P. Popper, Acta Cryst. **11**, 54–55 (1958).
[9]R. J. D. Tilley, J. Solid State Chem. **21**, 293–301 (1977).
[10]R. J. D. Tilley, Nature **269**, 229–231 (1977).
[11]A. Chernatynskiy, R. W. Grimes, M. A. Zurbuchen, D. R. Clarke, and S. R. Phillpot, Appl. Phys. Lett. **95**, 161906 (2009).
[12]S. Ohta, T. Nomura, H. Ohta, and K. Koumoto, J. Appl. Phys. **97**, 034106 (2005).
[13]J. Ravichandran, W. Siemons, D.-W. Oh, J. T. Kardel, A. Chari, H. Heijmerikx, M. L. Scullin, A. Majumdar, R. Ramesh, and D. G. Cahill, Phys. Rev. B **82**, 165126 (2010).
[14]C. Yu, M. L. Scullin, M. Huijben, R. Ramesh, and A. Majumdar, Appl. Phys. Lett. **92**, 191911 (2008).
[15]K. H. Lee, S. W. Kim, H. Ohta, and K. Koumoto, J. Appl. Phys. **100**, 063717 (2006).
[16]Y. Wang, K. H. Lee, H. Ohta, and K. Koumoto, J. Appl. Phys. **105**, 103701 (2009).
[17]D.-W. Oh, J. Ravichandran, C.-W. Liang, W. Siemons, B. Jalan, C. M. Brooks, M. Huijben, D. G. Schlom, S. Stemmer, L. W. Martin, A. Majumdar, R. Ramesh, and D. G. Cahill, Appl. Phys. Lett. **98**, 221904 (2011).
[18]E. Breckenfeld, R. Wilson, J. Karthik, A. R. Damodaran, D. G. Cahill, and L. W. Martin, Chem. Mater. **24**, 331–337 (2012).
[19]See supplementary material at http://dx.doi.org/10.1063/1.4927200 for growth and measurement details.
[20]G. E. Stillman and C. M. Wolfe, Thin Solid Films **31**, 69–88 (1976).
[21]T. L. Peterson, F. Szmulowicz, and P. M. Memenger, J. Cryst. Growth **106**, 16–33 (1990).
[22]D. G. Schlom and L. N. Pfeiffer, Nat. Mater. **9**, 881–883 (2010).
[23]Note that the specific coefficient of the thermal conductivity tensor being measured is k_{33}, corresponding to the coefficient describing the heat flow parallel to the direction of the applied temperature gradient (both are along the direction perpendicular to the substrate surface). This nomenclature is analogous to the definition of "longitudinal stress," "longitudinal strain," "longitudinal piezoelectric effect," and analogous tensor quantities. See, for example, J. F. Nye, *Physical Properties of Crystals: Their Representation by Tensors and Matrices* (Oxford University Press, 1957, 1985), pp. **127**, 144.
[24]J. H. Haeni, C. D. Theis, D. G. Schlom, W. Tian, X. Q. Pan, H. Chang, I. Takeuchi, and X.-D. Xiang, Appl. Phys. Lett. **78**, 3292–3294 (2001).
[25]K. Kuroda, K. Kojima, M. Tanioku, K. Yokoyama, and K. Hamanaka, Jpn. J. Appl. Phys., Part 1 **28**, 1586–1592 (1989).
[26]J. Fujita, T. Tatsumi, T. Yoshitake, and H. Igarashi, Appl. Phys. Lett. **54**, 2364–2366 (1989).
[27]H.-U. Krebs and M. Kehlenbeck, Physica C **162–164**, 119–120 (1989).
[28]K. Kojima, D. G. Schlom, K. Kuroda, M. Tanioku, K. Hamanaka, J. N. Eckstein, and J. S. Harris, Jr., Jpn. J. Appl. Phys., Part 2 **29**, L1638–L1641 (1990).
[29]D. G. Schlom, A. F. Marshall, J. T. Sizemore, Z. J. Chen, J. N. Eckstein, I. Bozovic, K. E. von Dessonneck, J. S. Harris, Jr., and J. C. Bravman, J. Cryst. Growth **102**, 361–375 (1990).
[30]H.-U. Krebs, M. Kehlenbeck, M. Steins, and V. Kupcik, J. Appl. Phys. **69**, 2405–2409 (1991).
[31]S. Hendricks and E. Teller, J. Chem. Phys. **10**, 147–167 (1942).
[32]G. Grzinic, Philos. Mag. A **52**, 161–187 (1985).
[33]R. Seshadri, M. Hervieu, C. Martin, A. Maignan, B. Domenges, B. Raveau, and A. N. Fitch, Chem. Mater. **9**, 1778–1787 (1997).
[34]C. M. Brooks, L. Fitting Kourkoutis, T. Heeg, J. Schubert, D. A. Muller, and D. G. Schlom, Appl. Phys. Lett. **94**, 162905 (2009).
[35]B. Jalan, R. Engel–Herbert, N. J. Wright, and S. Stemmer, J. Vac. Sci. Technol., A **27**, 461–464 (2009).
[36]T. Ohnishi, K. Shibuya, T. Yamamoto, and M. Lippmaa, J. Appl. Phys. **103**, 103703 (2008).
[37]K. Shibuya, S. Mi, C. Jia, P. Meuffels, and R. Dittmann, Appl. Phys. Lett. **92**, 241918 (2008).
[38]S. Madhavan, D. G. Schlom, A. Dabkowski, H. A. Dabkowska, and Y. Liu, Appl. Phys. Lett. **68**, 559–561 (1996).
[39]D. G. Schlom, S. B. Knapp, S. Wozniak, L-N. Zou, J. Park, Y. Liu, M. E. Hawley, G. W. Brown, A. Dabkowski, H. A. Dabkowska, R. Uecker, and P. Reiche, Supercond. Sci. Technol. **10**, 891–895 (1997).
[40]Y. Jia, M. A. Zurbuchen, S. Wozniak, A. H. Carim, D. G. Schlom, L-N. Zou, S. Briczinski, and Y. Liu, Appl. Phys. Lett. **74**, 3830–3832 (1999).
[41]R. Takahashi, K. Valset, E. Folven, E. Eberg, J. K. Grepstad, and T. Tybell, Appl. Phys. Lett. **97**, 081906 (2010).
[42]T. Ohnishi and K. Takada, Appl. Phys. Express **4**, 025501 (2011).
[43]M. Uchida, Y. F. Nie, P. D. C. King, C. H. Kim, C. J. Fennie, D. G. Schlom, and K. M. Shen, Phys. Rev. B **90**, 075142 (2014).
[44]C. H. Lee, N. D. Orloff, T. Birol, Y. Zhu, V. Goian, E. Rocas, R. Haislmaier, E. Vlahos, J. A. Mundy, L. F. Kourkoutis, Y. Nie, M. D. Biegalski, J. Zhang, M. Bernhagen, N. A. Benedek, Y. Kim, J. D. Brock, R. Uecker, X. X. Xi, V. Gopalan, D. Nuzhnyy, S. Kamba, D. A. Muller, I. Takeuchi, J. C. Booth, C. J. Fennie, and D. G. Schlom, Nature **502**, 532–536 (2013).
[45]C. H. Lee, N. J. Podraza, Y. Zhu, R. F. Berger, S. Shen, M. Sestak, R. W. Collins, L. F. Kourkoutis, J. A. Mundy, H. Q. Wang, Q. Mao, X. X. Xi, L. J. Brillson, J. B. Neaton, D. A. Muller, and D. G. Schlom, Appl. Phys. Lett. **102**, 122901 (2013).
[46]Y. Tokuda, S. Kobayashi, T. Ohnishi, T. Mizoguchi, N. Shibata, Y. Ikuhara, and T. Yamaoto, Appl. Phys. Lett. **99**, 173109 (2011).
[47]T. Suzuki, Y. Nishi, and M. Fujimoto, Philos. Mag. A **80**, 621–637 (2000).
[48]S. Wiedigen, T. Kramer, M. Feuchter, I. Knorr, N. Nee, J. Hoffmann, M. Kamlah, C. A. Volkert, and C. Jooss, Appl. Phys. Lett. **100**, 061904 (2012).
[49]R. A. De Souza, J. Fleig, R. Merkle, and J. Maier, Z. Metallkd. **94**, 218–225 (2003).
[50]H. Muta, K. Kurosaki, and S. Yamanaka, J. Alloys Compd. **392**, 306–309 (2005).
[51]T. Ohnishi, M. Lippmaa, and T. Yamamoto, Appl. Phys. Lett. **87**, 241919 (2005).
[52]C.-H. Lee, Y. Zhu, Q.-Y. Mao, J. A. Mundy, D. A. Muller, X. X. Xi, D. G. Cahill, D. G. Schlom, and M. A. Zurbuchen (unpublished).
[53]R. M. Costescu, D. G. Cahill, F. H. Fabreguette, Z. A. Sechrist, and S. M. George, Science **303**, 989–990 (2004).
[54]J. Ravichandran, A. K. Yadav, R. Cheaito, P. B. Rossen, A. Soukiassian, S. J. Suresha, J. C. Duda, B. M. Foley, C. H. Lee, Y. Zhu, A. W. Lichtenberger, J. E. Moore, D. A. Muller, D. G. Schlom, P. E. Hopkins, A. Majumdar, R. Ramesh, and M. A. Zurbuchen, Nat. Mater. **13**, 168–172 (2014).
[55]K. H. Lee, Y. F. Wang, S. W. Kim, H. Ohta, and K. Koumoto, Int. J. Appl. Ceram. Technol. **4**, 326–331 (2007).
[56]W. Sugimoto, M. Shirata, M. Takemoto, S. Hayami, Y. Sugahara, and K. Kuroda, Solid State Ionics **108**, 315–318 (1998).
[57]D. G. Schlom, Y. Jia, L.-N. Zou, J. H. Haeni, S. Briczinski, M. A. Zurbuchen, C. W. Leitz, S. Madhavan, S. Wozniak, Y. Liu, M. E. Hawley, G. W. Brown, A. Dabkowski, H. A. Dabkowska, R. Uecker, and P. Reiche, Proc. SPIE **3481**, 226–240 (1998).
[58]Z. Wang, M. Okude, M. Saito, S. Tsukimoto, A. Ohtomo, M. Tsukada, M. Kawasaki, and Y. Ikuhara, Nat. Commun. **1**, 106 (2010).